On the ionization energies of C4H3 isomers

Ralf I. Kaiser [a,*], Alexander Mebel [b], Oleg Kostko [c], Musahid Ahmed [c]

[a] University of Hawaii at Manoa, Department of Chemistry, Honolulu, HI 96822, United States
[b] Florida International University, Department of Chemistry, Miami, FL 33199, United States
[c] Chemical Sciences Division, Lawrence Berkeley National Laboratory, Berkeley, CA 94720, United States

ARTICLE INFO

ABSTRACT

We have investigated the ionization potentials of resonantly stabilized C_4H_3 radicals utilizing laser abla-tion of graphite in combination with seeding the ablated species in neat methylacetylene gas, which also reacted as a reagent. Photoionization efficiency (PIE) curves were recorded of photoionized isomers at the Advanced Light Source. The PIE curve suggests the formation of four C_4H_3 radicals: two acyclic structures i-C_4H_3 [**1**] and E/Z-n-C_4H_3 [**2E/2Z**] and two cyclic isomers **3** and **4**. This study provides a novel interpre-tation of previous data on C_4H_3 radicals in hydrocarbon flames.

© 2009 Elsevier B.V. All rights reserved.

1. Introduction

Resonantly stabilized free radicals (RSFRs) such as propargyl (C_3H_3; $HCCCH_2$; X^2B_1) and 1-buten-3-yn-2-yl (C_4H_3; $HCCCCH_2$; X^2A'), in which the unpaired electron is delocalized across the car-bon skeleton, are considered as central reaction intermediates to form polycyclic aromatic hydrocarbons (PAHs) in combustion flames [1–3] and in the interstellar medium [4,5]. Whereas it is well established that the propargyl isomer presents an exclusive open shell isomer among the C_3H_3 radicals detected in hydrocar-bon flames [6–8], the situation is far from being resolved for the C_4H_3 isomers. The photoionization curves, i.e. a plot of the ioniza-tion energy versus the count rates of the C_4H_3 ion at $m/z = 51$ was measured from analysis of propyne and allene flames photoionized with tunable VUV synchrotron radiation. These studies suggested the existence of at least the i-C_4H_3 isomer [9], which is thermody-namically favorable by 44 ± 2 kJ mol^{-1} compared to the n-C_4H_3 structure [10]. An adiabatic ionization energies of the i-C_4H_3 iso-mer of 8.06 ± 0.05 eV was derived. Because of low Franck–Condon factors, the authors suggested that their sensitivity with respect to the n-C_4H_3 isomer was limited. Chemical dynamics experiments exploiting the crossed molecular beam method showed that C_4H_3 radicals can be formed under single collision conditions as a product of bimolecular reactions. These involve reactions of ground state carbon atoms ($C(^3P_j)$) with methylacetylene (CH_3CCH) [11] and allene (H_2CCCH_2) [12] as well as bimolecular collisions of dicarbon in its ground and first electronically excited states, i.e. $C_2(X^1\Sigma_g^+)$ and $C_2(a^3\Pi_u)$, with ethylene (H_2CCH_2); these processes lead to the synthesis of the C_s symmetric i-C_4H_3 isomer:

$HCCCCH_2(X^2A')$. The n-C_4H_3 isomer ($HCCCHCH$; X^2A') was identified as a reactive intermediate formed in the initial addition of the ethynyl radical (CCH) to acetylene (HCCH). However, a de-tailed analysis of the center-of-mass functions as extracted from the crossed beam reactions of ground state carbon atoms with methylacetylene [11] suggested that an elusive high-energy iso-mer, might have also been synthesized. The molecular structure of this isomer is still unknown.

Which approach could be applied to unravel the structure of potential high-energy C_4H_3 isomers? For distinct structural iso-mers, the adiabatic ionization energy (IE) can differ significantly. Here, the adiabatic ionization energy presents a measurable quantity of the energy required to remove an electron from a molecule in its rotational, vibrational, and electronic ground state hence forming a cation in its lowest electronic, vibrational, and rotational level. The adiabatic ionization energy presents one of the most relevant thermochemical measurements: ionization energies cannot only be utilized to determine the nature of the structural isomers, i.e. of hydrocarbon radicals, but they can be combined with thermochemical cycles to obtain enthalpies of formation of hydrocarbon radicals. This method was applied suc-cessfully to derive the ionization energies of highly reactive or-ganic transient radicals like linear and cyclic C_3H to be 9.15 and 9.76 eV, respectively [13]. Here, we synthesize multiple C_4H_3 isomers in a supersonic molecular beam via laser ablation of a graphite rod followed by *in situ* reaction of the ablated car-bon atoms with methylacetylene. The neutral radicals in this supersonic beam are then photoionized by vacuum ultraviolet (VUV) light from the Advanced Light Source at various photon energies. Based on electronic structure calculations, the recorded photoionization efficiency curves are then simulated theoreti-cally to extract the adiabatic ionization energies of the C_4H_3 isomers.

---

* Corresponding author.
  E-mail address: ralfk@hawaii.edu (R.I. Kaiser).

2. Theoretical methods

Geometries of various C_4H_3 isomers and their ions have been optimized using the hybrid density functional B3LYP method [14,15] with the 6-311G** basis set. In general, this approach is known to be reliable for geometric parameters. For example, the bond lengths and bond angles optimized at the B3LYP/6-311G** level for Z-n-C_4H_3 and E-n-C_4H_3 coincide with those obtained by Wheeler et al. [16] by more sophisticated CCSD(T)/TZ(2d1f,2p1d) calculations within 0.01 Å and 1°, respectively. However, the i-C_4H_3 isomer is an exception. B3LYP calculations gave for this isomer a C_{2v}-symmetric structure with a linear C_4 fragment, on the contrary to the results of higher level calculations [17]. Therefore, we used the CCSD(T)/6-311G** optimized C_s-symmetric geometry for i-C_4H_3, which again is in a close agreement with the CCSD(T)/TZ(2d1f,2p1d) results of Wheeler et al. [16]. For consistency, geometry of the i-$C_4H_3^+$ cation was also optimized at the CCSD(T)/6-311G** level; however, in this case the CCSD(T) and B3LYP geometries are very close. Vibrational frequencies were computed at B3LYP/6-311G**, except for i-C_4H_3 and its cation, for which the CCSD(T)/6-311G** method was employed. To refine vertical and adiabatic ionization energies of various C_4H_3 isomers, we performed coupled cluster CCSD(T) calculations [18–21] with extrapolation to the complete basis set (CBS) limit. To achieve this, we computed CCSD(T) total energies for each neutral and cationic C_4H_3 species with Dunning's correlation-consistent cc-pVDZ, cc-pVTZ, cc-pVQZ, and cc-pV5Z basis sets [22] and projected them to CCSD(T)/CBS total energies by fitting the following equation [23]:

$$E_{tot}(x) = E_{tot}(\infty) + Be^{-Cx}, \qquad (1)$$

where x is the cardinal number of the basis set (2, 3, 4, and 5, respectively) and $E_{tot}(\infty)$ is the CCSD(T)/CBS total energy. All ab initio calculations were carried out using the GAUSSIAN 98 [24] and MOLPRO 2006 [25] program packages. Franck–Condon factors calculations for the C_4H_3 ionization processes have been performed in harmonic approximation using a model of displaced and distorted harmonic oscillators [26,27] and utilizing molecular structures and vibrational frequencies of the neutral and ion species obtained from the ab initio calculations.

3. Experimental methods

The experiments were conducted at the Chemical Dynamics Beamline of the Advanced Light Source at Lawrence Berkeley National Laboratory. The C_4H_3 isomers were formed in situ within a laser ablation source [13]. Here, about 2 mJ of the 532 nm output of a Neodymium–Yttrium–Aluminum–Garnet (Nd:YAG) laser were focused to a 1 mm spot onto a rotating graphite rod (99.995%, Aldrich). The ablated species were then seeded in methylacetylene (99+%; Aldrich) carrier gas, which was released by a Proch–Trickl pulsed valve operating at a stagnation pressure of 135 kPa and repetition rate of 50 Hz. The methylacetylene carrier gas also acted as a reactant to form multiple C_4H_3 radicals in situ. Tunable VUV light from the Advanced Light Source crossed the neutral molecular beam 120 mm downstream of the ablation center and 65 mm after the skimmer in the extraction region of a Wiley–McLaren time-of-flight (TOF) mass spectrometer. The ions of the photoionized molecules were extracted and collected by a microchannel plate detector in the TOF mode utilizing a multichannel scaler. The photoionization efficiency (PIE) curves can be obtained by plotting the integrating the $C_4H_3^+$ signal at mass-to-charge, m/z, of 51 versus the photoionization energy between 8.0 and 10.3 eV in steps of 0.1 eV. The signal was normalized to the photon flux. These PIE curves can be exploited to extract the adiabatic ionization energies of the radicals [13].

4. Results and discussion

First, we would like to comment on the structures of low lying C_4H_3 isomers together with their cations. Hereafter, the ionization energies are discussed to aid an interpretation of the photoionization curve obtained for the C_4H_3 ions at $m/z = 51$. The optimized geometries of the neutral C_4H_3 isomers and their cations in the lowest singlet and triplet states are illustrated in Fig. 1. For the present consideration, we have chosen five lowest in energy C_4H_3 structures [17], i-C_4H_3 **1**, E and Z conformations of n-C_4H_3 **2E** and **2Z**, as well as two cyclic isomers **3** and **4**. i-C_4H_3 **1** represents the most stable structure, with n-C_4H_3 conformers residing ∼0.5 eV higher in energy and **3** and **4** being 1.32 and 1.42 eV less favorable than **1**, respectively. Note that the energy difference between i-C_4H_3 and n-C_4H_3 calculated here closely matches the previous high-level results by Wheeler et al. [16]. Ionization of **1** is found to significantly change its geometry. In particular, the symmetry of the molecule increases from C_s to C_{2v} as the C_4 chain becomes linear in the ion, both in the singlet (**1s$^+$**) and (**1t$^+$**) triplet electronic states. CCSD(T) calculations of neutral **1** and ionized **1s$^+$** and **1t$^+$** (both at the vertical and optimized geometries) gave T1 diagnostic values [28,29] of 0.022, 0.024–0.025, and 0.031–0.037, respec-
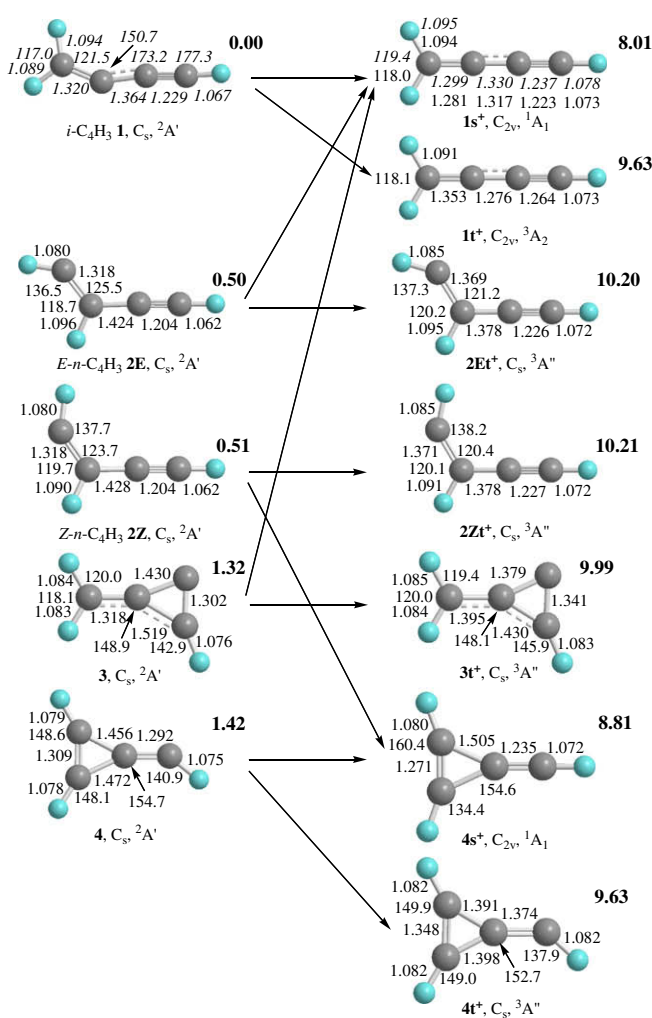
Fig. 1. Geometries of neutral and ionic C_4H_3 isomers optimized at the B3LYP/6-311G** (plain numbers) and CCSD(T)/6-311G** (italics) levels of theory. Bond lengths are given in Å and bond angles in °. Symmetry point groups and electronic states are also shown. Bold numbers give relative energies of the neutral and ionic species (in eV) with respect to i-C_4H_3 **1** calculated at the CCSD(T)/CBS level of theory. Arrows show the directions of geometry relaxation after ionization.

Table 1
Calculated vertical and adiabatic ionization energies (in eV) of various C_4H_3 isomers.

	i-C_4H_3, **1**		E-n-C_4H_3, **2E**		Z-n-C_4H_3, **2Z**		**3**		**4**	
Ion state[a]	$^1A'$ ($^1A_1$)	$^3A''$ ($^3A_2$)	$^1A'$ ($^1A_1$)[b]	$^3A''$ ($^3A''$)	$^1A'$ ($^1A_1$)[c]	$^3A''$ ($^3A''$)	$^1A'$ ($^1A_1$)[b]	$^3A''$ ($^3A''$)	$^1A'$ ($^1A_1$)	$^3A''$ ($^3A''$)
Vert. IE	8.46	9.84	9.77	9.85	9.79	9.87	9.45	9.00	8.25	8.57
Adiab. IE	8.01	9.63	7.51	9.70	8.30	9.70	6.69	8.67	7.39	8.21

[a] Electronic state of the cation at the geometry of the neutral C_4H_3 species and at the geometry optimized for the cation (in parentheses).
[b] Geometry optimization of the cation converges to **1s$^+$**.
[c] Geometry optimization of the cation converges to **4s$^+$**.

tively, indicating only a moderate multireference character of the wave functions for these species, which means that their energies should be accurately described by the CCSD(T) method. Noteworthy that the ionization process producing the singlet ion differs from that to form the triplet state. In the former case, an electron is removed from the singly occupied a' molecular orbital of i-C_4H_3, but in the latter case from the underlying doubly occupied a'' orbital. This is general for all C_4H_3 isomers considered here and explains the calculated differences between the energetics of singlet and triplet $C_4H_3^+$. Since the singlet $^1A_1$ electronic state is much lower in energy than triplet $^3A_2$ (Table 1), we performed Franck–Condon factor calculations for $^1A_1$. The geometry relaxation in **1s$^+$** as compared to **1** involves shortening of some C–C bonds by up to 0.03 Å, whereas CCC angles increase by up to 30°. These changes are reflected in significant displacements of several vibrational normal modes, which in turn result in small Franck–Condon factors with ionization peaks spread over a broad energy range (see Supporting Information). The calculated adiabatic ionization energy, 8.01 eV, is 0.45 eV lower than the vertical IE (Table 1) and the ionization spectrum of **1** is predicted to represent a broad continuum originated at ∼8 eV with slowly increasing intensity that can be spread as far as to the 10–11 eV energy range.

Although the n-C_4H_3 structures have vertical IEs to singlet ionic states slightly lower than those to the triplet states of the ion, the geometry relaxation in singlets is drastic; the **2Es$^+$** and **2Zs$^+$** structures optimize to C_{2v}-symmetric H_2CCCCH^+ (**1s$^+$**) and cyclic **4s$^+$**, respectively, starting from the equilibrium geometries of the neutral species. This means that Franck–Condon factors for ionization of n-C_4H_3 to singlet ionic states should be unfavorable. On the other hand, ionization to the triplet ionic states results to relatively minor geometric changes and is expected to give rise to short series of distinct peaks in the spectra. As seen in Table 1 and in Supporting Information, the series of ionization peaks due to **2Et$^+$**($^3A''$) ← **2E**($^2A'$) and **2Zt$^+$**($^3A''$) ← **2Z**($^2A'$) starts at ∼9.7 eV and is spread to ∼10.2 eV, with the origin peaks being the most intense. The cyclic C_4H_3 isomer **3** at the vertical geometry has a ground triplet $^3A''$ ionic state, whereas the singlet $^1A'$ state is 0.45 eV higher in energy. Geometry relaxation of the singlet ion leads to the linear **1s$^+$** structure, which should result in very unfavorable Franck–Condon factors. Alternatively, geometry changes from **3** to the triplet **3t$^+$** ion are rather moderate and Franck–Condon factor calculations give a series of distinct peaks with the origin at 8.67 and spreading over to ∼9.9 eV (Supporting Information); the ionization peaks at 8.67 and 9.07 eV are predicted to be the most intense. The second cyclic isomer **4** has vertical IPs of 8.25 and 8.57 eV to singlet and triplet states, respectively. Geometry relaxation in the singlet state is more significant as the symmetry changes from C_s to C_{2v} with the out-of-ring CCH group becoming linear. Similar to **1**, we can expect the **4s$^+$** ← **4** ionization spectra to be a broad featureless continuum with the origin at 7.39 eV. Ionization to the triplet state, **4t$^+$**($^3A''$) ← **4**($^2A'$), leads to moderate structural changes and the calculated Franck–Condon factors show a progression of separate ionization peaks, where the intensity of the origin peak at 8.21 eV by far exceeds intensities of the others. Calculated T1 diagnostic values, 0.019 for **4**, 0.025–0.031 for **4s$^+$**, and 0.018–0.021 for **4t$^+$**, show
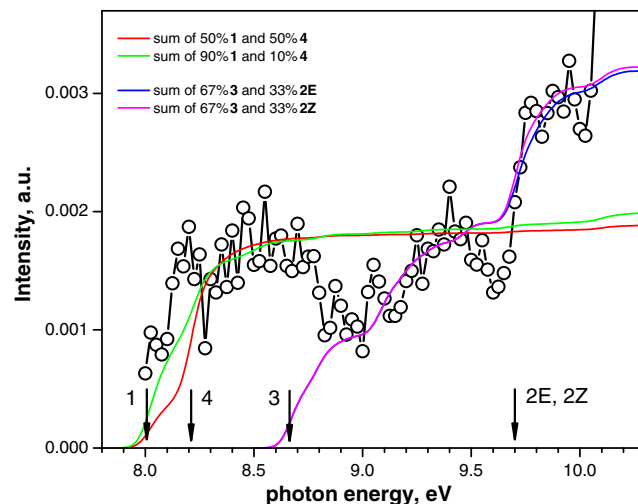
Fig. 2. Photoionization efficiency curve for C_4H_3 isomers recorded at m/z = 51. Open circles correspond to experimental data. Arrows represent positions of adiabatic ionization energy for various C_4H_3 isomers as compiled in Table 1.

that these species are expected to be properly described by the CCSD(T) method applied in the present calculations.

Having tackled the molecular structures of the C_4H_3 neutrals and their ions as well as the ionization energies and the inherent Franck–Condon factors, we are turning our attention now to the experimental data obtained. Here, a scan of the photon energy allows for extraction of a photoionization efficiency (PIE) curve, which is shown in Fig. 2. The signal originates at 8.0 eV rises sharply up to about 8.2 eV and then plateaus out at about 8.7 eV; hereafter, the signal drops down to about 9.0 eV. From 9.0 eV on, the signal rises again to about 9.4 eV, decreases significantly until 9.6 eV, and rises once again very steeply to about 10.0 eV. These experimental data can be compared with simulated PIE curves (Fig. 2). These simulated graphs are generated by convoluting the calculated FCFs with an 0.1 eV Gaussian function to simulate the light shape followed by integration. For the i-C_4H_3 isomer, the FCFs for different modes of the same energy were summed together. The red curve[1] shows a simulation of equal contribution from isomer **1** and **4**, whereas the green curve represents a 90% contribution of isomer **1** and 10% contribution of isomer **4**. It is clear that the simulated PIE reproduces both the adiabatic onset and also the general slope of the experimental data up to 8.7 eV. Therefore, our data suggest the existence of both the acyclic and cyclic isomers **1** and **4**, respectively. Likewise, this section of the PIE curve correlates nicely with the computed ionization energy of the i-C_4H_3 structure of 8.01 eV versus the experimental onset of about 8.0 eV to yield the C_{2v}-symmetric ion **1s$^+$** in its singlet state. As predicted theoretically, photo ionization of isomer **4** leads due to unfa-

---

[1] For interpretation of color in Figs. 1 and 2, the reader is referred to the web version of this article.
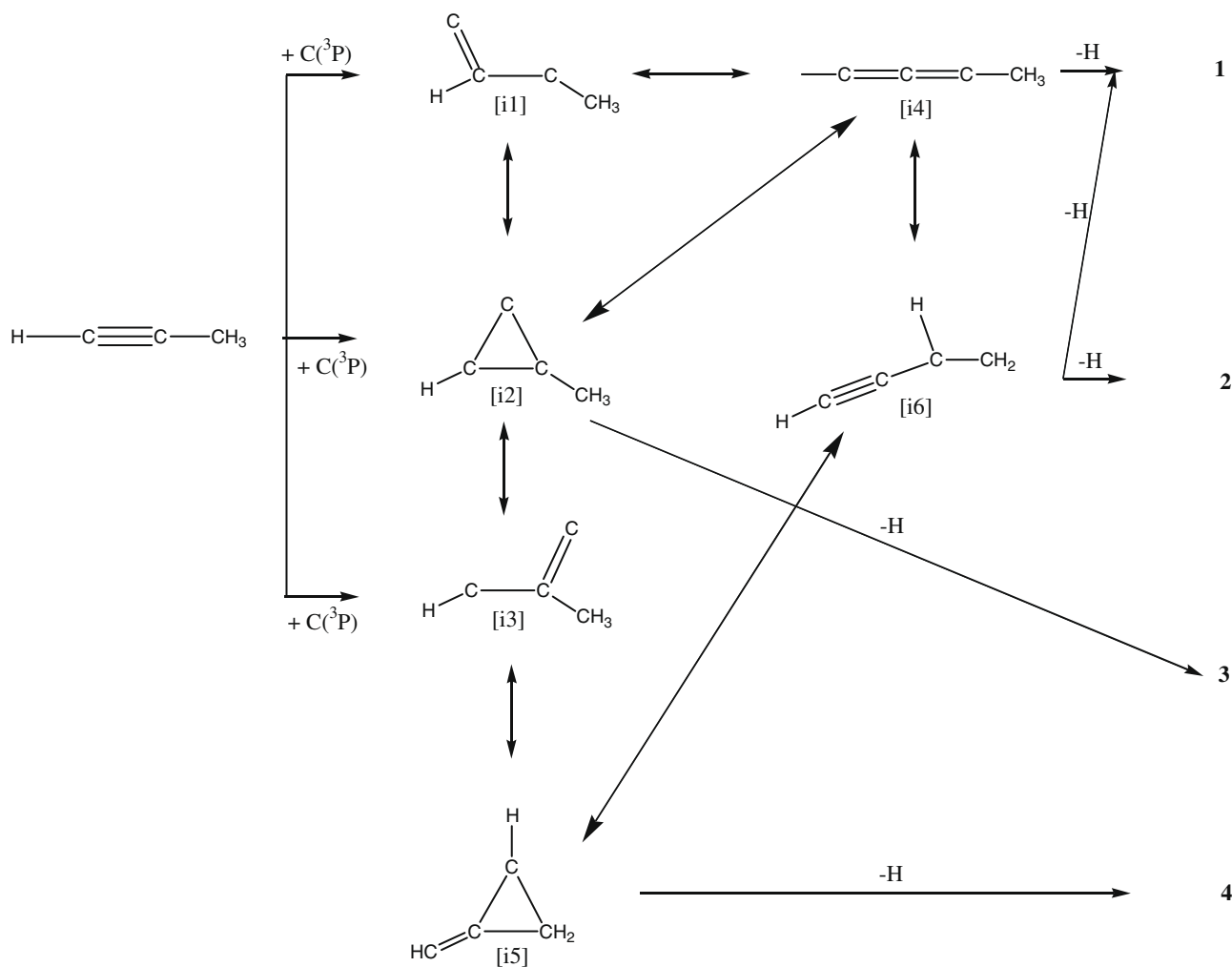
Fig. 3. Schematic representation of the formation of four C_4H_3 isomers via reaction of ground state carbon atoms with methylacetylene, isomerization of the initial collision complexes, and decomposition of distinct intermediates to form multiple C_4H_3 structures.

vorable FCFs to **4t⁺**, but not to **4s⁺**; this is also reflected in the absence of any signal at $m/z = 51$ below 8.0 eV. If **4s⁺** was formed, we would have expected ion counts starting at about 7.4 eV, which were clearly not observed. To summarize, the section of the PIE curve from 8.0 to 8.7 eV indicates the formation of an acyclic and cyclic C_4H_3 isomer in the supersonic beam: **1** and **4**. In a similar manner, the blue graph presents a simulated PIE curve for a 67% contribution from isomer **3** and 33% contribution from isomer **2E**; the magenta curve shows a contribution of 33% from the **2Z** isomer. Again it is apparent that the calculated PIEs broadly reproduce the shape of PIE curve in the 9.0–10.0 eV region suggesting that isomer **3** as well as **2E/2Z** are present in the beam. Note that the dips at 9.0 eV and 9.7 eV are likely caused from autoionization or from dissociative ionization of the neutral precursors at higher photon energies. In the absence of absolute photoionization cross-sections, we shall stress that the assumed contributions of various isomers to the derived PIE allows for only a qualitative analysis of the population of isomers in the beam.

How can the isomers be formed? Theoretically, the reaction mechanism was suggested based on electronic structure calculations of the triplet C_4H_4 PES [30]. Upon reaction of laser ablated ground state carbon atoms, the latter could add to the carbon–carbon double bond of the methylacetylene molecule to form intermediates [i1], [i2], and/or [i3] (Fig. 3). Structure [i1] could isomerize to [i2] via ring closure or undergoes hydrogen migration to [i4]. Alternatively, [i3] could ring-close to [i2] or [i5]; in the

latter case the ring closure is accompanied with a 1,2-H shift. [i2] and [i5] could ring-open to yield [i4] and [i6], respectively. A hydrogen migration in [i4] can connect this structure to isomer [i6]. These intermediates can undergo unimolecular decomposition via atomic hydrogen loss to form the experimentally detected products **1** (from [i4] to [i6]), **2** (from [i6]), **3** (from [i2]), and **4** (from [i5]).

For completeness, we would like to discuss if the C_4H_4 intermediates [i1] to [i6] (Fig. 3) can undergo dissociative photodissociation to form $C_4H_3^+$ plus atomic hydrogen. Table 2 compiles the calculated appearance energies. It is important to note that only [i4] and [i6] can serve as precursors to the $C_4H_3^+$ cations **1** and **4**; [i2] is a precursor of **3**, and [i5] presents a precursor of isomer **4**. All these relevant energies given in italics are higher than 9.72–9.76 eV. Therefore, dis-

Table 2
Calculated appearance energies (eV) of various $C_4H_3^+$ structures from dissociative photoionization of different triplet C_4H_4 isomers **i1–i6**.

	i1	i2	i3	i4	i5	i6
1s⁺ + H	7.59	8.46	7.46	10.04	8.92	*9.76*
1t⁺ + H	9.21	10.08	9.09	*11.66*	10.54	*11.39*
2Et⁺ + H	9.78	10.65	9.65	12.23	11.11	*11.96*
2Zt⁺ + H	9.79	10.66	9.66	12.24	11.12	*11.96*
3t⁺ + H	9.57	*10.44*	9.44	12.02	10.90	11.74
4s⁺ + H	8.39	9.26	8.26	10.84	*9.72*	10.56
4t⁺ + H	9.21	10.08	9.09	11.66	*10.54*	11.39

sociative ionization may contribute only around 10 eV and higher energies, but not at lower energies. Therefore, we do not have to take into account signal at $m/z = 51$ from dissociative photoionization of the C_4H_4 intermediates [i1] to [i6] at energies lower than 10 eV.

5. Conclusions

Our combined experimental and theoretical study suggested the synthesis of four C_4H_3 radicals in a supersonic beam generated via laser ablation of graphite and seeding the ablated species in neat methylacetylene, which also acted as a reagent. These are two acyclic radicals i-C_4H_3 [**1**] and E/Z-n-C_4H_3 [**2E/2Z**] and two cyclic structures **3** and **4**. Note that previous flame studies only suggested the formation of the thermodynamically most stable i-C_4H_3 isomer [9]. The different product spectra could be the result of a combination of distinct production methods of the radicals (supersonic beams versus combustion flames) and different pressure conditions in the flame and within the supersonic expansion. Further, the present experiments support the prediction from previous crossed molecular beam studies of ground state carbon atom with methylacetylene at lower collision energies that a higher energy C_4H_3 isomer, possibly of cyclic structure, likely contributes to reactive scattering signal [11].

Acknowledgment

Appendix A. Supplementary material

Supplementary data associated with this article can be found, in the online version, at doi:10.1016/j.cplett.2009.12.027.

References

[1] J.A. Miller, S.J. Klippenstein, J. Phys. Chem. A 107 (2003) 7783.
[2] Y. Georgievskii, A. Miller James, J. Klippenstein Stephen, Phys. Chem. Chem. Phys. 9 (2007) 4259.
[3] A.M. Herring, J.T. McKinnon, D.E. Petrick, K.W. Gneshin, J. Filley, B.D. McCloskey, J. Anal. Appl. Pyrol. 66 (2003) 165.
[4] O. Morata, E. Herbst, Mon. Not. Roy. Astron. Soc. 390 (2008) 1549.
[5] C. Boersma, A.L. Mattioda, C.W. Bauschlicher Jr., E. Peeters, A.G.G.M. Tielens, L.J. Allamandola, Astrophys. J. 690 (2009) 1208.
[6] T. Zhang et al., J. Chem. Phys. 124 (2006) 074302/1.
[7] J. Wang et al., J. Phys. Chem. A 112 (2008) 9255.
[8] Y. Li, L. Zhang, Z. Tian, T. Yuan, J. Wang, B. Yang, F. Qi, Energy Fuels 23 (2009) 1473.
[9] N. Hansen et al., J. Phys. Chem. A 110 (2006) 3670.
[10] D. Domin, W.A. Lester Jr., R. Whitesides, M. Frenklach, J. Phys. Chem. A 112 (2008) 2065.
[11] R.I. Kaiser, D. Stranges, Y.T. Lee, A.G. Suits, J. Chem. Phys. 105 (1996) 8721.
[12] R.I. Kaiser, A.M. Mebel, A.H.H. Chang, S.H. Lin, Y.T. Lee, J. Chem. Phys. 110 (1999) 10330.
[13] R.I. Kaiser, L. Belau, S.R. Leone, M. Ahmed, Y. Wang, B.J. Braams, J.M. Bowman, Chem. Phys. Chem. 8 (2007) 1236.
[14] A.D. Becke, J. Chem. Phys. 98 (1993) 5648.
[15] C. Lee, W. Yang, R.G. Parr, Phys. Rev. B: Condensed Matter Mater. Phys. 37 (1988) 785.
[16] S.E. Wheeler, W.D. Allen, H.F. Schaefer III, J. Chem. Phys. 121 (2004) 8800.
[17] T.N. Le, A.M. Mebel, R.I. Kaiser, J. Comput. Chem. 22 (2001) 1522.
[18] G.D. Purvis III, R.J. Bartlett, J. Chem. Phys. 76 (1982) 1910.
[19] G.E. Scuseria, C.L. Janssen, H.F. Schaefer III, J. Chem. Phys. 89 (1988) 7382.
[20] G.E. Scuseria, H.F. Schaefer III, J. Chem. Phys. 90 (1989) 3700.
[21] J.A. Pople, M. Head-Gordon, K. Raghavachari, J. Chem. Phys. 87 (1987) 5968.
[22] T.H. Dunning Jr., J. Chem. Phys. 90 (1989) 1007.
[23] K.A. Peterson, T.H. Dunning Jr., J. Phys. Chem. 99 (1995) 3898.
[24] M.J. Frisch et al., GAUSSIAN 98, Revision A5, Gaussian, Inc., Pittsburgh, PA, 1998.
[25] H.-J. Werner et al., MOLPRO, version 2006.1, a package of ab initio programs, <http://www.molpro.net>.
[26] A.M. Mebel, Y.-T. Chen, S.-H. Lin, Chem. Phys. Lett. 258 (1996) 53.
[27] A.M. Mebel, Y.-T. Chen, S.-H. Lin, J. Chem. Phys. 105 (1996) 9007.
[28] T.J. Lee, P.R. Taylor, J. Quantum Chem., Quantum Chem. Symp. 23 (1989) 199.
[29] C.J. Cramer, Essentials of Computational Chemistry: Theories and Models, Wiley, Chichester, 2002.
[30] A.M. Mebel, R.I. Kaiser, Y.T. Lee, J. Am. Chem. Soc. 122 (2000) 1776.